Shihui Guo[a], Peter Briza, Viktor Magdolen, Hans Brandstetter and Peter Goettig*

Activation and activity of glycosylated KLKs 3, 4 and 11

https://doi.org/10.1515/hsz-2018-0148
Received February 1, 2018; accepted June 21, 2018; previously published online July 5, 2018

Abstract: Human kallikrein-related peptidases 3, 4, 11, and KLK2, the activator of KLK3/PSA, belong to the prostatic group of the KLKs, whose major physiological function is semen liquefaction during the fertilization process. Notably, these KLKs are upregulated in prostate cancer and are used as clinical biomarkers or have been proposed as therapeutic targets. However, this potential awaits a detailed characterization of these proteases. In order to study glycosylated prostatic KLKs resembling the natural proteases, we used *Leishmania* (LEXSY) and HEK293 cells for secretory expression. Both systems allowed the subsequent purification of soluble pro-KLK zymogens with correct propeptides and of the mature forms. Periodic acid-Schiff reaction, enzymatic deglycosylation assays, and mass spectrometry confirmed the glycosylation of these KLKs. Activation of glycosylated pro-KLKs 4 and 11 turned out to be most efficient by glycosylated KLK2 and KLK4, respectively. By comparing the glycosylated prostatic KLKs with their non-glycosylated counterparts from *Escherichia coli*, it was observed that the *N*-glycans stabilize the KLK proteases and change their activation profiles and their enzymatic activity to some extent. The functional role of glycosylation in prostate-specific KLKs could pave the way to a deeper understanding of their biology and to medical applications.

Keywords: enzyme kinetics; eukaryotic expression; *N*-linked glycosylation; prostate cancer biomarker; zymogen activation.

[a]Present address: The Institute of Oceanography, Minjiang University, Xiyuan Gong Road 200, Minhou, Fuzhou, Fujian 350108, People's Republic of China.
***Corresponding author: Peter Goettig,** Division of Structural Biology, Department of Biosciences, University of Salzburg, Billrothstrasse 11, A-5020 Salzburg, Austria, e-mail: peter.goettig@sbg.ac.at. http://orcid.org/0000-0002-2430-1970
Shihui Guo, Peter Briza and Hans Brandstetter: Division of Structural Biology, Department of Biosciences, University of Salzburg, Billrothstrasse 11, A-5020 Salzburg, Austria
Viktor Magdolen: Klinische Forschergruppe der Frauenklinik, Klinikum rechts der Isar der TU München, Ismaninger Str. 22, D-81675 München, Germany

Introduction

Among the 15 human kallikrein-related peptidases two subgroups in male and female reproductive organs and fluid secretions exhibit a rather complementary expression pattern on the RNA and protein level: KLKs 2, 3, 4 and 11 are mostly detected in testis, prostate and semen, while KLKs 6, 7, 8, 10, 12 and 13 are mainly present in uterus, vagina and cervico-vaginal fluid (Harvey et al., 2000; Shaw and Diamandis, 2007; Uhlén et al., 2015). Prostatic KLKs fulfill important tasks in impregnation, in particular KLK2 and KLK3/PSA digest the gel-forming proteins semenogelin I and II, which liquefies the seminal clot and increases the motility of spermatozoa (Sotiropoulou et al., 2009; Emami and Diamandis, 2012). Although KLK11 does not cleave semenogelins, it may activate KLKs 2 and 3, whereby KLK2 seems to be the major activator of KLK3 (Lovgren et al., 1997; Luo et al., 2006). KLKs 3 and 11 could be activators of KLK4 by cleaving the unusual propeptide SCSQ-I^{16}ING (Yoon et al., 2007). Similarly, the role of KLK4 in semen liquefaction is not entirely clear and might be the degradation of extracellular matrix (ECM) proteins, such as fibronectin (Matsumura et al., 2005). Under pathological conditions, KLK4 appears to adopt a more prominent role by degradation of ECM proteins and, possibly, by activation of matrix metalloproteinase-1 (MMP-1), which is believed to be critical for tumor cell invasion and metastasis (Fuhrman-Luck et al., 2016). In addition, the prostatic KLKs 2, 3, 4 and 11 can cleave insulin-like growth factor binding protein IGFBP3 and activate urokinase-type plasminogen activator uPA, as well as proteinase-activated receptors PAR1 and PAR2, which are expressed at much higher levels in prostate cancer tissues than in benign and normal prostate tissues (Avgeris et al., 2012; Fuhrman-Luck et al., 2014). Apart from uPA, KLK4 can also directly cleave uPAR and thereby modulate the activity of the uPA/uPAR system (Beaufort et al., 2006).

Despite a less crucial role in prostate cancer, the enhanced expression and concomitantly enhanced serum levels rendered KLK3 as prostate specific antigen the most relevant prognostic biomarker based on an immunoassay (Papsidero et al., 1980; Kuriyama et al., 1981). In order to achieve a better distinction between malignant and benign forms of prostate cancer, various KLK3 forms,

including pro-KLK3 plus KLK2, KLK4 and KLK11 have been tentatively used as prognostic markers, which improved the quality of prognosis significantly in some approaches (Stephan et al., 2007; Gupta et al., 2010; Hong, 2014). Recent studies corroborated that KLK4 levels in seminal plasma and blood serum have no prognostic value for prostate cancer patients, whereas KLK4 participates in the protease network, which is responsible for the dissemination of metastasizing prostate cancer cells (Karakosta et al., 2016; Reid et al., 2017).

Approximately 50% of human proteins are *N*- and/or *O*-glycosylated, mostly representing secreted soluble proteins or integrated membrane proteins with their extracellular regions (Apweiler et al., 1999). All KLKs possess potential *N*-glycosylation sites at asparagine in so-called sequons, such as Asn-Xaa-Ser/Thr (NXS/T), with Xaa being usually not Pro, whereas *O*-glycosylation takes place at Ser or Thr in Pro-rich regions without a distinct consensus sequence (Guo et al., 2014). In addition, non-consensus sequons, such as NXC, NGX and NXV can be *N*-glycosylated, but the degree of glycosylation varies as for standard sequons, depending on the three-dimensional (3D) protein architecture, whereby surface loops are strongly favored as glycosylation sites (Zielinska et al., 2010; Aebi, 2013). Structure-function analyses of glycan-free and glycosylated KLK2 demonstrated that the single core-glycan at Asn95 in the kallikrein/99-loop near the active site suffices to regulate the activation, enzymatic activity and deactivation (Figure 1A) (Skala et al., 2014; Guo et al., 2016). Similarly, KLK3 possesses a single *N*-glycan at Asn61, whose role has not been revealed yet, while additional *O*-glycosylation has been reported for KLK3 at Thr125 (Figure 1B) (Stura et al., 2011). The KLK4 sequence contains a potential *N*-glycosylation site at Asn159, which is also present in the mouse and pig homologs mKlk4 and pKLK4, linked to variable multiantennary *N*-glycans, besides additional *N*-glycans attached to Asn120 and Asn202 (Figure 1C) (Yamakoshi et al., 2011). The sequence of KLK11 contains two sequons corresponding to the glycosylation sites at Asn159 and Asn202, while it possesses two additional sequons at Asn95 and Asn175 (Guo et al., 2014). Glycosylation *in vivo* has been confirmed for several KLKs and has attracted growing attention, as the effects of glycosylation are widespread and critical in the life cycle of many proteases from expression to regulation of activity and their degradation (Goettig, 2016).

Aberrant glycosylation has been observed in a variety of diseases, especially in various cancer types, such as in

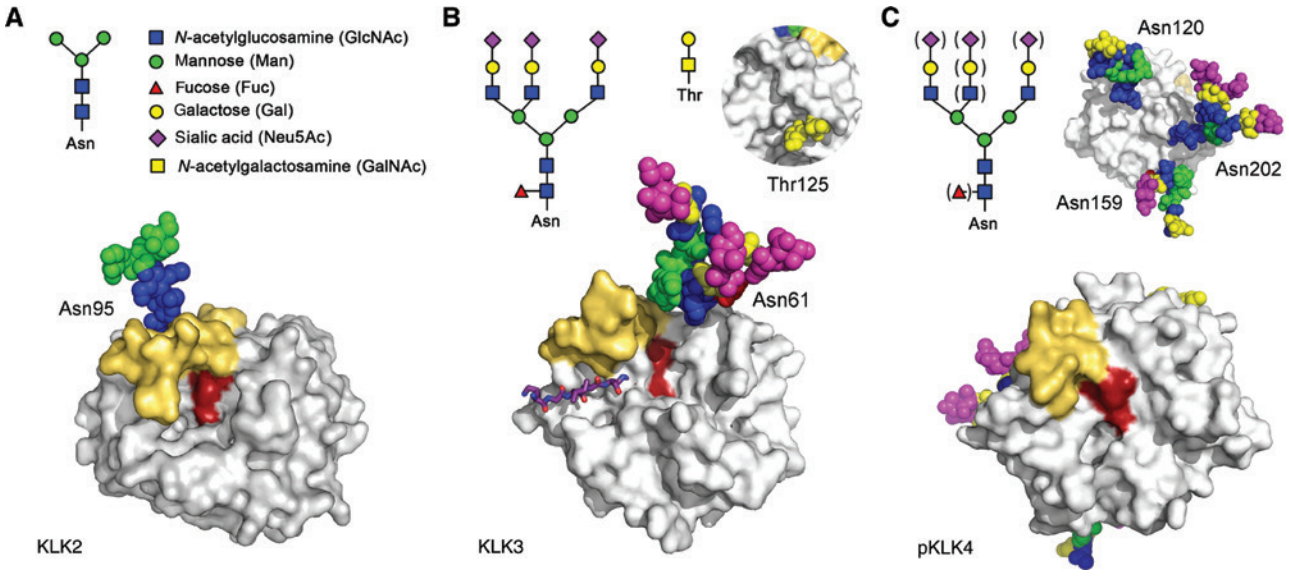

Figure 1: Comparison of glycosylated prostatic KLKs as surface representation.
Glycans are depicted as spheres and color symbols according to standard nomenclature. (A) Human KLK2 from *Leishmania* expression exhibits a small *N*-linked core glycan of the $GlcNAc_2Man_3$ type. The presence of this glycan at Asn95 in the 99-loop (yellow) of $KLK2_{lx}$ reduced the substrate turnover significantly compared to glycan-free $KLK2_e$, by favoring a closed stated of the active site. Catalytic triad residues are shown as dark red patches. (B) Natural KLK3/PSA as observed in a crystal structure (PDB code 3QUM), exhibiting a complex triantennnary glycan at Asn61, with terminal sialic acids units, often Neu5Ac (magenta). The 99-loop is in an open state allowing access of substrates, e.g. shown as stick model bound to the non-prime side. Opposite to the active site, an *O*-glycan is linked to Thr125, which consists of GalNAc-Gal (insert). (C) Porcine pKLK4 is linked to three multiantennary *N*-glycans at Asn120, Asn159 and Asn202, with varying branching and length (Yamakoshi et al., 2011). The role of these glycans is still unknown, although they seem important for folding and stability.

prostate cancer for KLK3/PSA (Tabares et al., 2006; Sarrats et al., 2010). Glycosylated KLK3 expressed by the prostate tumor cell line LNCaP was remarkably different from KLK3 present in seminal plasma (Peracaula et al., 2003). The carbohydrate component of glyco-KLK3 from healthy individuals exclusively exhibits α-2,6 sialic acid, whereas that from PCa patients was mainly α-2,3 sialic acid (Yoneyama et al., 2014). The altered glycosylation pattern appears to be a predictive marker for discrimination between aggressive and non-aggressive cancers and may allow for a personalized medicine approach (Gilgunn et al., 2013; Padler-Karavani, 2014; Drake et al., 2015). However, full use of such an approach awaits detailed *in vitro* studies accompanied by information on biological and pathological functions of KLKs. Since protein glycosylation has a remarkable influence on folding, stability, molecular recognition, activity, specificity and regulation, it is worth investigating the effects of glycosylation on KLKs 3, 4 and 11, in order to obtain a more complete picture, which was outlined before with glycosylated KLK2 (Guo et al., 2016).

Results

Eukaryotic expression of proforms and mature glyco-KLKs 3, 4, 11

Secretory expression of prostatic kallikrein-related peptidases in eukaryotic cells was chosen, in order to obtain folded and glycosylated proteins, resembling the natural human KLKs. The variants will be designated according to their expression origin as KLK_{lx} (LEXSY), KLK_S or KLK_T (HEK293S/T) and KLK_e (*Escherichia coli*). Expression of native-like pro-KLK3 constructs in *Leishmania* (LEXSY) and HEK293T cells was not sufficient. Both HEK293T and S cells produced larger amounts of the construct for mature KLK3 comprising an artificial propeptide with an N-terminal His-tag and an enterokinase (EK) cleavage site, exhibiting a molecular mass of about 30 kDa on sodium dodecyl sulfate (SDS) gels after EK digest (data not shown).

By contrast, pro-KLK4 constructs were successfully expressed in LEXSY and HEK293T with N-terminal His-tags. After TEV protease digest, the native-like pro-$KLK4_{lx}$ form was obtained as a stable zymogen. N-terminally His-tagged KLK4 with EK cleavages sites were expressed in LEXSY and HEK293T cells with higher yields. According to SDS gels, activated mature $KLK4_T$ had a molecular weight around 28 kDa, while $KLK4_{lx}$ displayed a molecular weight slightly above 26 kDa (data not shown).

Expression of pro-KLK11 in HEK293T and LEXSY cells with the legumain (AEP) cleavage site His_6-GSN-ETR-I[16] was feasible and purified samples of pro-$KLK11_{lx}$ were rather stable. LEXSY and HE293 cells expressed sufficient amounts of mature KLK11 with an artificial His-tag propeptide. After EK digest, mature $KLK11_{lx}$ showed a double band around 34 kDa in SDS gels, indicating slightly inhomogeneous glycosylation (data not shown).

Characterization of glycosylated KLKs 3, 4, 11

Edman degradation confirmed the correct N-terminal sequences IINGDCYP and IIKGFECK of the LEXSY expressed $KLK4_{lx}$ and $KLK11_{lx}$, respectively. In addition, the IVGGWECEKHS N-terminal sequences of KLK3 from $HE293_{S/T}$ cells were confirmed, as the corresponding sequences of the $KLK4_T$ construct. Glycan staining with the periodic acid-Schiff reaction (PAS) indicated that all investigated samples of KLKs 3, 4, and 11 were glycosylated to some extent (data not shown).

Also, $KLK3_T$ with an artificial propeptide and His6-tag, exhibited a molecular weight of about 32 kDa on SDS gels, which shifted roughly to 28 kDa upon treatment with PNGase F, while Endo Hf treatment resulted in weaker bands around 30 kDa, indicating the presence of a complex, multiantennary *N*-glycan (Figure 2A). The sequon around Asn61 is the only predicted *N*-glycosylation site of KLK3, which was confirmed by a crystal structure (Stura et al., 2011). However, mass spectrometric analysis of KLK3 glycosylation was inconclusive, probably due to inhomogeneous *N*-glycosylation or loss of glycosylated peptides in the experiment.

Enzymatic deglycosylation for LEXSY and HEK293T cell expressed KLK4 was only successful with PNGase F, whereby the shift for $KLK4_{lx}$ was about 1 kDa and more than 2 kDa for $KLK4_T$ to about 26 kDa. The predicted *N*-glycosylation site at Asn159 was glycosylated according to mass spectrometry, as peptides in tryptic and chymotryptic digests carried a small core glycan of 892.32 Da in case of $KLK4_{lx}$ and a larger one of 1216.42 Da in case of $KLK4_T$ (Figure 2B). Most likely, the first one is a $GlcNAc_2Man_3$ core known for *Leishmania* glycosylation, while the second one comprises two more hexoses, e.g. GlcNAc and galactose, or mannose of a hybrid glycan. Peptides from tryptic digest showed smaller fractions of unpredicted additional *N*-glycans, which were not linked to standard sequons (N^{95}RP, N^{101}DL), with N^{202}GY exhibiting the highest degree of glycosylation (Figure 2B).

The apparent molecular weight of $KLK11_{lx}$ was roughly 36 kDa, which is significantly higher than the expected

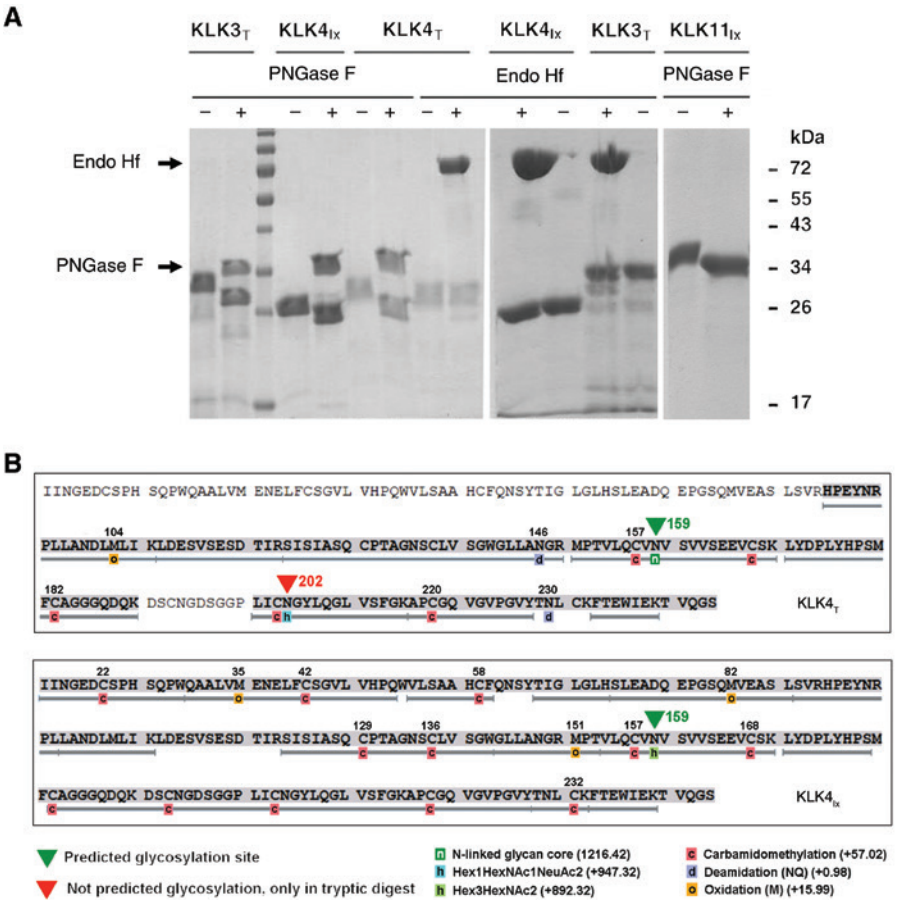

Figure 2: Characterization of glycosylated prostatic KLKs.
(A) SDS gel of KLKs 3, 4 and 11 treated with deglycosylating enzymes. PNGase F cleaved glycans of $KLK3_T$, $KLK4_T$, $KLK4_{lx}$ and $KLK11_{lx}$. PNGase F removes Asn-linked GlcNAc in general, while Endo Hf cleaves between two GlcNAc, requiring mannose-rich glycans (Freeze and Kranz, 2010). Endo Hf leaves complex $KLK4_{lx}$ *N*-glycans intact, whereas some deglycosylation of $KLK3_T$ and $KLK4_T$ is observed. PNGase F removed only a fraction of $KLK11_{lx}$ glycans. (B) Mass spectrometric analysis of peptide coverage after tryptic and chymotryptic digest of glycosylated KLK4 samples. The *N*-glycosylation site at Asn159 (green triangle) was confirmed for both KLK_{lx} as core glycan (h), corresponding most likely to $GlcNAc_2Man_3$, and as more complex glycan for $KLK4_T$ peptides (n). A not predicted glycosylation at Asn202 in $KLK4_T$ was only present in a fraction of peptides from tryptic digest with an overall relatively low score. Other modifications originate from technical procedures (c, carbamidomethylation) or chemical reactions (d, o).

26 kDa for the unmodified protein. PNGase F treatment resulted only in a minor shift on SDS gels to about 34 kDa. Mass spectrometry indicates only partial glycosylation of Asn95, Asn159 and Asn175, in contrast to Asn202, which carried a core glycan of 892.32 Da, corresponding to $GlcNAc_2Man_3$. In particular, peptides containing Asn95 exhibited a significant glycan-free fraction. Moreover, these glycosylation sites could be glycosylated with more variations than the one at Asn202, for which an additional acetylation seems possible. Thr161 and Ser204, belonging to the sequons at Asn159 and Asn202, respectively, might be linked to *O*-glycans, which was not clearly resolved, whereas a comparable *O*-glycosylation pattern at sequons has been reported for human KLK1 (Kellermann et al., 1988).

Pro-KLKs 3, 4 and 11 activation

As prostate-specific KLKs have a three to seven residue propeptide, the additional residues in the N-terminal His-tag and protease recognition sequence may allow detecting molecular weight shifts upon analysis by SDS-polyacrylamide gel electrophoresis (PAGE). The two available fusion proteins pro-KLK4lx with His_6-GS-ENLYFQ-SCSQ-↓-IINGEDC[22] and pro-KLK11lx with His_6-GS-N-ETR-↓-IIKGFEC[22] were incubated with mature prostatic KLKs at 37°C for 24 h. The activating cleavage at the scissile peptide bonds of pro-KLK4 and pro-KLK11 at Gln-Ile[16] and Arg-Ile[16] require a modified chymotryptic and a regular tryptic activator protease, respectively. The properly activated zymogens of KLK4 and KLK11 will result

in mature proteases with trypsin-like activity. Beside SDS-PAGE detection, the tryptic activity of these samples was determined to quantify the amount of activated species. From the activity assay, $KLK2_{lx}$ and $KLK2_{e}$ showed the strongest activation of pro-KLK4, followed by $KLK11_{lx}$. This finding seems inconsistent with previous reports, indicating that KLK11 and KLK3 are the only members of the KLK family, which can process propeptides with Gln in the P1 position (Yoon et al., 2007). Surprisingly, the best activator for KLK4 seemed to be KLK2, which usually has a strong preference for P1-Arg residues (Cloutier et al., 2002; Skala et al., 2014). Apparently, the *N*-glycosylation of $KLK2_{lx}$ nearly doubles the activation efficiency (Figure 3A).

Activation of pro-KLK11 with Arg15 at the P1 position requires tryptic proteases such as KLK2, 4 and 11, rather than the chymotryptic KLK3 (Figure 3B). Glycosylated $KLK2_{lx}$ was more active in pro-KLK11 activation than the corresponding non-glycosylated $KLK2_{e}$ and comparable to $KLK4_{T}$. A further 30% increase in activation efficiency was observed for the KLKs with glycosylation of the LEXSY type compared with the one of the HEK293 cell type. $KLK4_{lx}$ proved to be the best activator of pro-KLK11 (Figure 3B). Due to the low zymogen activity of pro-KLK11, auto-activation was not observed at all over 24 h.

Enzymatic activity and inhibition of glycosylated KLKs 3, 4 and 11

Several chromogenic and fluorogenic substrates were tested with the various glycosylated prostatic KLKs and non-glycosylated counterparts from *E. coli* expression, in order to assess the influence of the glycans on the enzymatic activity. A comparison for glycosylated $KLK2_{lx}$ with $KLK2_{e}$ revealed significant differences in enzyme kinetic parameters and processing of large proteins (Guo et al., 2016). $KLK3_{S}$ and $KLK3_{T}$ preferred chymotryptic substrates, e.g. Suc-AAF-AMC, and showed activity stimulation with 20 mM citrate and inhibition by 20 μM Zn^{2+}, as it was reported for KLK3 from *E. coli* and insect cell expression (Hsieh and Cooperman, 2000; Andrade et al., 2010). In contrast to the chymotryptic KLK3, glycosylated $KLK4_{lx}$, $KLK4_{T}$ and $KLK11_{lx}$ strongly preferred tryptic substrates, such as Bz-PFR-pNA, while the chymotryptic H-AAF-AMC was not cleaved (data not shown).

A systematic investigation of the three glycosylated prostatic KLKs was carried out and whenever possible compared to the activity of the non-glycosylated KLK_{e} variant. The same substrates were used for the respective KLKs, in order to obtain comparable Michaelis constants (K_M values). Proper determination of k_{cat} values and the catalytic efficiency was based on active site titration for each sample. Overall, the glycosylated KLK variants exhibited higher fractions of active proteases, as it was already observed for $KLK2_{e}$ and $KLK2_{lx}$ (Guo et al., 2016). For example, $KLK4_{e}$ and $KLK11_{e}$ were only 7% and 14% active, whereas their glycosylated counterparts $KLK4_{lx}$ and $KLK11_{lx}$ were 48.5 and 73% active, indicating a stabilizing effect of the various glycans. Interestingly, $KLK4_{e}$ and $KLK4_{lx}$ have nearly equal K_M (536 μM and 635 μM) for the substrate Suc-AAPR-pNA, but the k_{cat} of $KLK4_{e}$ (0.89 s^{-1}) is significantly lower than the one of $KLK4_{lx}$ (1.99 s^{-1}), which resembles the situation for KLK11 (Table 1). In case of $KLK11_{e}$ and $KLK11_{lx}$ with Bz-IEGR-pNA

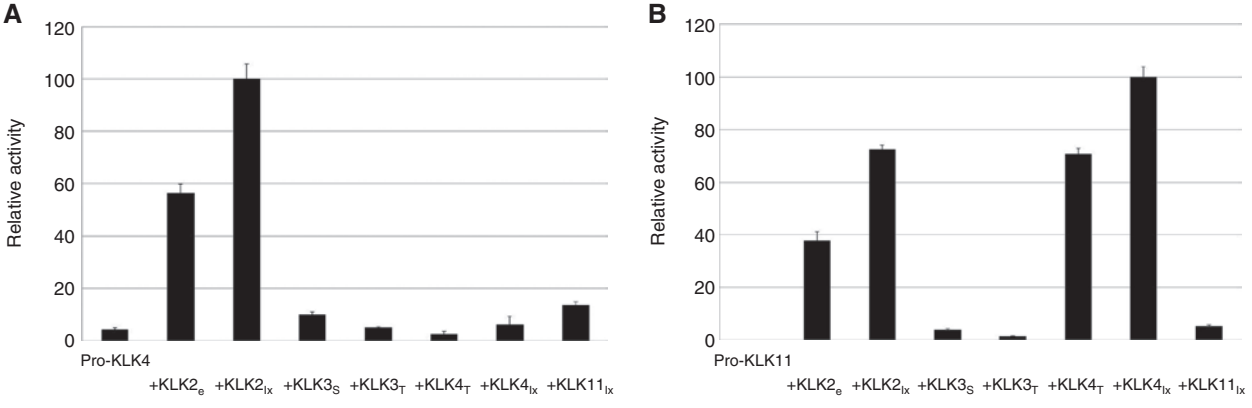

Figure 3: Activation of pro-KLKs 4 and 11.
Ten micrograms pro-KLK were incubated with 0.1 μg protease and the presented activity against H-PFR-AMC was measured. Controls with activating proteases alone showed no activity. (A) Pro-KLK4 shows a little autoactivation and activation by $KLK4_{lx}$ and $KLK4_{T}$. Moderate activation is seen with $KLK3_{S/T}$ and $KLK11_{lx}$, which might be relevant in physiological processes. However, the best activators were $KLK2_{e}$ and $KLK2_{lx}$ despite the rather unusual cleavage site at the Gln15-Ile16 bond. (B) Both KLK2 variants activate pro-KLK11 very well, while the best activator was $KLK4_{lx}$. By contrast, $KLK3_{S/T}$ were weak activators of pro-KLK11, which does not autoactivate or significantly activate as mature $KLK11_{lx}$.

Table 1: Enzyme kinetic parameters for glycan-free and glycosylated prostatic KLKs determined by Michaelis-Menten kinetics.

KLK	Substrate	K_M (μM)	k_{cat} (s^{-1})	k_{cat}/K_M ($M^{-1} \cdot s^{-1}$)	IC_{50} Zn^{2+}
$KLK3_S$	Suc-AAPF-pNA	1486 ± 408	0.033 ± 0.004	22 ± 7	17 μM
$KLK3_T$	Suc-AAPF-pNA	n.d.	n.d.	n.d.	n.d.
$KLK4_e$	Suc-AAPR-pNA	536 ± 139	0.89 ± 0.08	1660 ± 456	34 μM
$KLK4_{lx}$	Suc-AAPR-pNA	635 ± 51	1.99 ± 0.03	3134 ± 256	15 μM
$KLK4_T$	Suc-AAPR-pNA	n.d.	n.d.	n.d.	n.d.
$KLK11_e$	Bz-IEGR-pNA	660 ± 150	1.52 ± 0.09	2303 ± 541	–
$KLK11_{lx}$	Bz-IEGR-pNA	820 ± 61	2.78 ± 0.08	3390 ± 270	–

For Michaelis constants K_M and turnover number k_{cat}, the weighted standard errors of the non-linear regression fitting were used, while the error of the catalytic efficiency was calculated according to the formula given by Fenner (1931). Active site titrations were performed for tryptic KLKs with PPACK in which $KLK11_e$ was 14% active, whereas the $KLK11_{lx}$ protein showed 73% activity. No significant inhibition was observed in the range 0–500 μM Zn^{2+} for both $KLK11_{lx}$ and $KLK11_e$. For KLK3S, the substrate Bz-AEPF-pNA was used. Errors are derived from experimentally measured and weighted data and given as standard deviations values.

only minor differences were observed in K_M (660 μM and 820 μM), however, the k_{cat} values (1.52 and 2.78 s^{-1}) differed by more than 50% as the resulting catalytic efficiencies (k_{cat}/K_M) (Figure 4A, Table 1). No comparison was possible for $KLK3_S$ with a $KLK3_e$ sample, since only the glycosylated variant exhibited a little turnover of the chymotryptic substrate Suc-AAPF-pNA with a high K_M (1.5 mM) and a low k_{cat} (0.033 s^{-1}), which is comparable to enzyme kinetic data from the literature (Watt et al., 1986). Apparently, Zn^{2+} does not inhibit both $KLK11_e$ and $KLK11_{lx}$ significantly, whereas the $KLK3_S$ activity was reduced by Zn^{2+} with an inhibition constant (IC_{50}) of 17 μM (Figure 4B, Table 1). This value is close to the reported 20 μM for natural seminal KLK3, as well as the 15% residual activity beyond 100 μM (Malm et al., 2000). Even around 500 μM Zn^{2+} $KLK4_{lx}$ has a residual activity of about 60%, with an apparent IC_{50} of 15 μM. Glycan-free $KLK4_e$ is more efficiently inhibited by Zn^{2+}, albeit with an elevated IC_{50} of 34 μM, showing a residual activity around 15% for 500 μM Zn.

Both glycosylated $KLK3_S$ and $KLK3_T$ processed the natural substrate fibronectin in a comparable manner, indicating that the different glycans may not affect their substrate specificity and turnover (Figure 5A). $KLK4_T$ and $KLK4_{lx}$ degraded fibronectin very rapidly, whereas $KLK11_{lx}$ cleaved it to a much lower extent (Figure 5A). Additionally, $KLK3_S$ and $KLK3_T$ formed SDS-stable complexes with natural inhibitors, such as the serpin α_1-antichymotrypsin (ACT), which is the primary

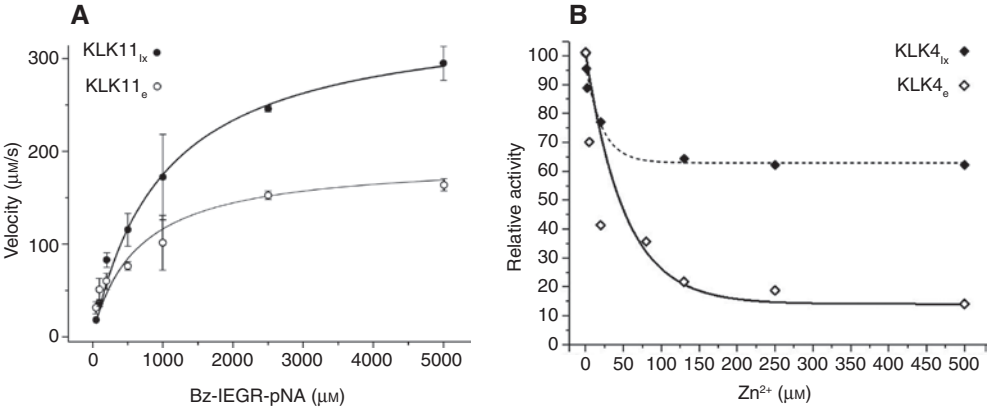

Figure 4: Enzyme kinetics of prostatic KLKs.
(A) Michaelis-Menten curve for $KLK11_{lx}$ compared to *E. coli* expressed KLK11. The turnover velocity in μM · s^{-1} has been normalized according to the active fractions of both enzymes, which was determined by active site titration with the irreversible inhibitor PPACK. The substrate Bz-Ile-Glu-Gly-Arg-pNA has a medium binding affinity, as corroborated by K_M of 660 and 820 μM for $KLK11_e$ and $KLK11_{lx}$, which are nearly the same when considering the error range. Apparently, the k_{cat} of 2.78 s^{-1} for $KLK11_{lx}$ (●) is 83% higher than the one of $KLK11_e$ (○). Also, $KLK4_e$ and $KLK4_{lx}$ did not exhibit strong differences in kinetic parameters. (B) Zn^{2+} inhibition of KLK4 variants. $KLK4_{lx}$ (◆) exhibits a high residual activity of about 60%, even around 500 μM Zn^{2+}, although the apparent inhibition constant IC_{50} is around 15 μM. By contrast $KLK4_e$ (◇) is much more efficiently inhibited by Zn^{2+}, albeit with a higher IC_{50} of 34 μM.

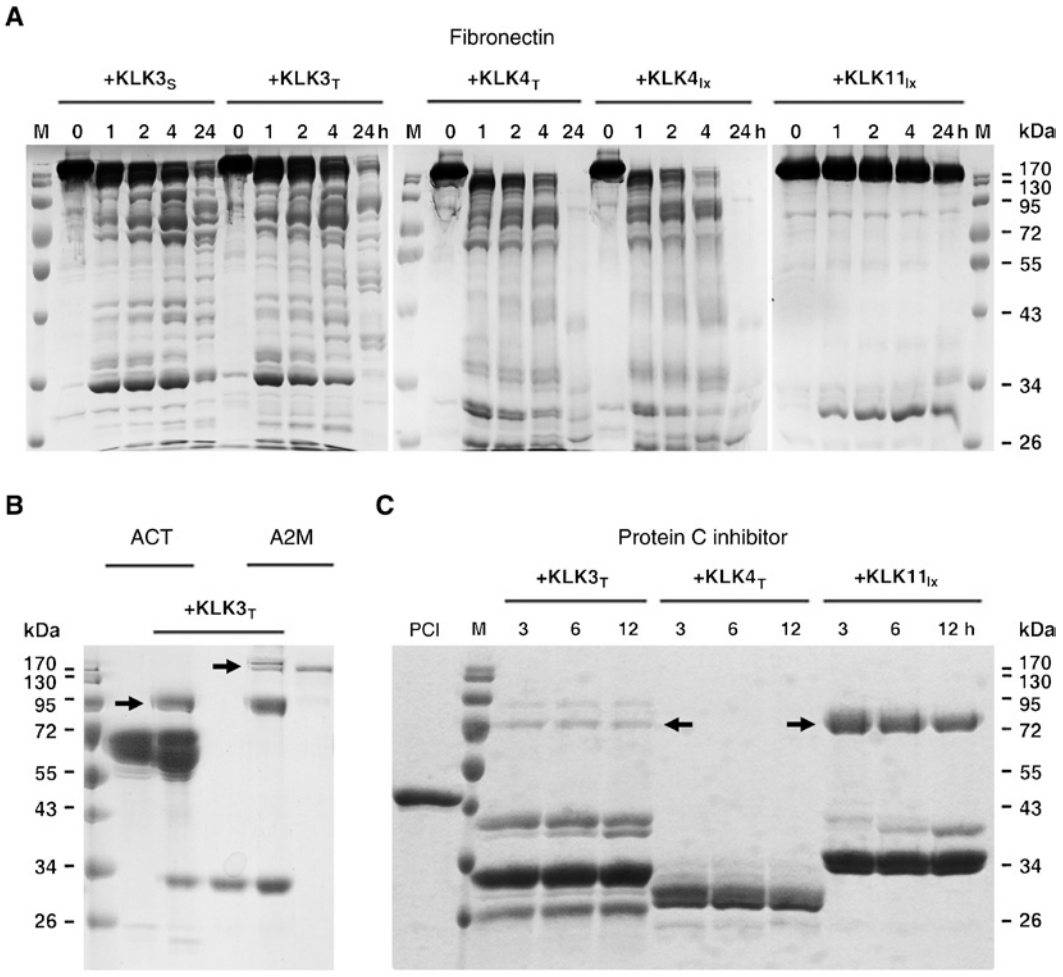

Figure 5: Turnover of fibronectin by various glycosylated KLKs 3, 4, and 11 and their interaction with physiological inhibitors.
(A) Fibronectin cleavage by KLKs 3, 4, and 11. The ratio of fibronectin to KLK4 and KLKL11 variants was 100:1, for KLK3 variants 20:1. The turnover was monitored over 24 h, whereby $KLK3_S$ and $KLK3_T$ degraded equally a large fraction of fibronectin (230 kDa band, left panel). $KLK4_T$ and $KLK4_{Ix}$ degraded fibronectin and its fragments nearly completely in a similar manner (middle panel). $KLK11_{Ix}$ left fibronectin nearly intact, except for cleaving off a 30 kDa fragment (right panel). (B) KLK3 complex formation with α_1-antichymotrypsin (ACT) and α_2-macroglobulin (A2M). The complex of ACT (65 kDa) with $KLK3_T$ is indicated by an arrow (3 h incubation). Only a small amount of $KLK3_T$ forms the complex (arrow) with A2M (180 kDa), while proteolytic cleavage of the inhibitor dominates, similar as for ACT. (C) Complex formation of the serpin PCI with $KLK3_T$, $KLK4_T$ and $KLK11_{Ix}$ at a molar ratio of 1:2 monitored over 12 h. Both $KLK3_T$ and $KLK4_T$ degraded recombinant PCI largely (46 kDa), whereby $KLK3_T$ was less efficient and even formed a small amount of stable complex (arrow). By, contrast, $KLK11_{Ix}$ bound most of the serpin inhibitor with very little degradation (arrow).

molecular form of serum KLK3, reaching up to 95% of total KLK3/PSA (Figure 5B) (Stenman et al., 1991). Seemingly, the different glycosylation patterns of KLK3 generated by HEK293S and T cells resemble the glycosylation variations of KLK3 isoforms A and B, which possesses more terminal sialic acids (Zhang et al., 1995). The reported slow KLK3-ACT complex formation *in vitro* was equally observed, whereby long incubation times resulted in liberation of KLK3 and increasing degradation of ACT as for natural KLK3 (Christensson et al., 1990). Similarly, the unspecific protease inhibitor α_2-macroglobulin (A2M), which is present in human serum, formed a complex with our recombinant $KLK3_T$ (Figure 5B). Moreover, the physiologically relevant complex formation with the protein C inhibitor (PCI) from the serpin family was confirmed for $KLK3_S$ and $KLK3_T$ (Figure 5C) (Christensson and Lilja, 1994). Whereas $KLK4_T$ degraded the PCI completely, an SDS-stable complex with PCI and $KLK11_{Ix}$ was formed, exhibiting an approximate molecular mass of 80 kDa (Figure 5C). This complex would be novel and might be relevant under physiological conditions in reproductive processes, as PCI complexes with an unspecified tissue kallikrein have been described in the literature (España et al., 2007).

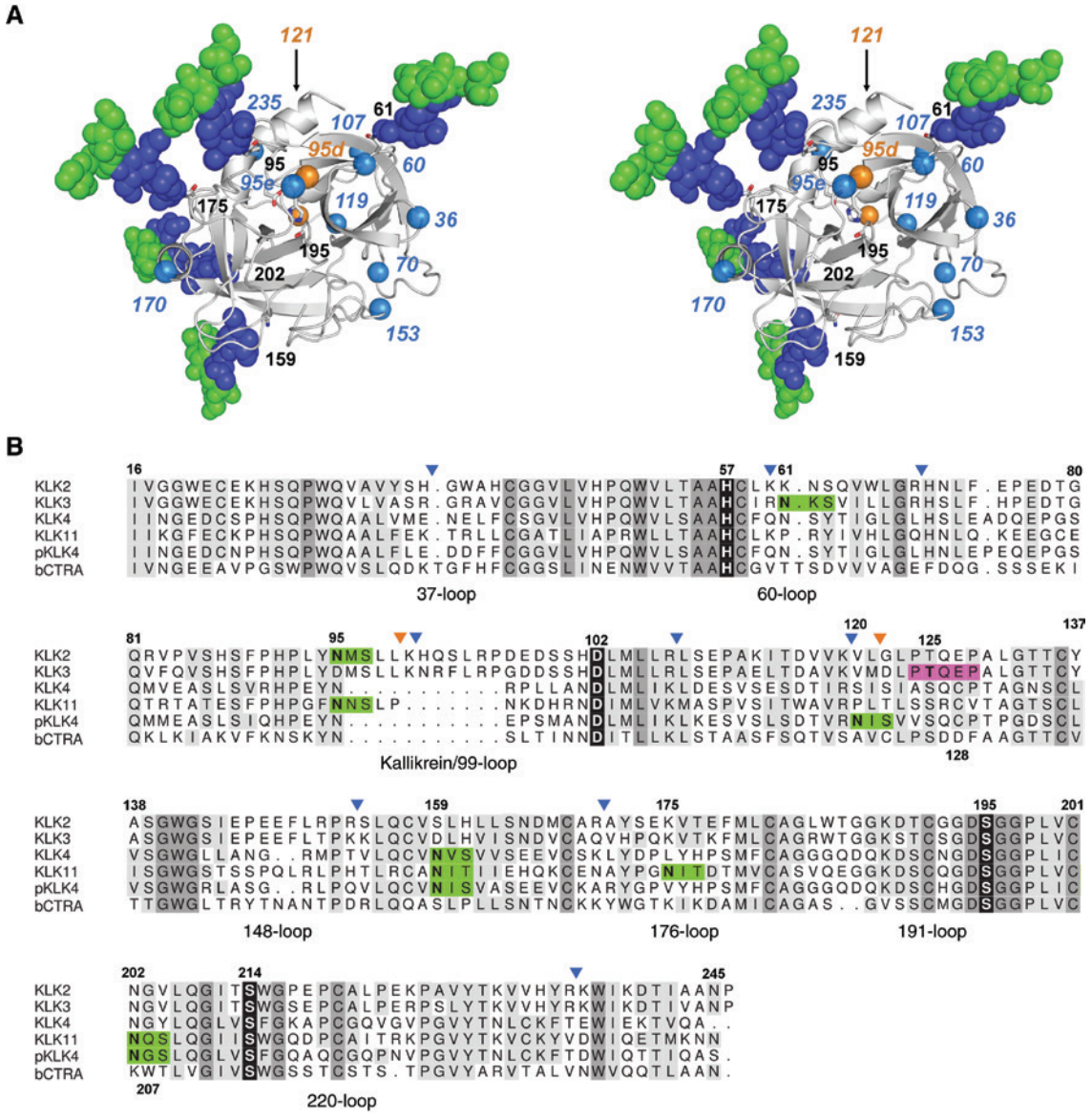

Figure 6: Structural model with cleavage sites and alignment of glycosylated prostatic KLKs.
(A) Position of glycosylation and cleavages site on a general ribbon model of KLKs 2, 3 4 and 11 in stereo. Black numbers designate known *N*-glycosylation sites at Asn residues, which are depicted with linked $GlcNAc_2Man_3$ core glycans. Exposed tryptic cleavages sites are shown as light blue spheres with corresponding labels, while the chymotryptic ones are shown in orange. Besides a role in proper folding, most of these *N*-glycans have the capacity to protect protease cleavage sites, which are mostly located in surface loops. An additional role in regulation of activity for the *N*-linked Glycan at Asn95 of KLK2 has been observed (Guo et al., 2016). (B) Sequence alignment of human KLKs 2, 3, 4, 11, porcine KLK4 and bovine chymotrypsin as numbering standard. The catalytic triad residues and Ser214 are highlighted with black background, as Ser214 can be considered as fourth residue of a catalytic tetrad (Engh et al., 1996). *N*-glycosylation sites are shown with green background, *O*-glycosylation sites with magenta background. Known tryptic and chymotryptic cleavage sites, which correspond to the ones shown in Figure 5A, are indicated by blue and orange triangles.

Discussion

Although the prostatic KLKs 2, 3, 4 and 11 are highly homologous, their expression as zymogens and mature proteases differs significantly in the three expression systems of *E. coli*, *Leishmania* and HEK293 cells according to our results (Skala et al., 2014). Expression of KLK3 in bacteria in bacteria is possible, but refolding from inclusion bodies is problematic, which can be explained by the requirement of the *N*-glycan at Asn61 for easy folding (Debela et al., 2006b). Similarly, expression of KLK5 failed completely in *E. coli*, whereas expression was successful in *Sf9* insect cells that generate small *N*-glycans (Debela et al., 2007). Otherwise, it is not clear, why KLK3 expression

was negligible in LEXSY cells, while KLK2 expression was preferred in this system, despite 80% identical sequences (Guo et al., 2016).

Since the type and extent of glycosylation, in particular the molecular weight differences, cannot be easily assessed by shifts on SDS gels upon deglycosylation, a thorough interpretation of the available mass spectrometry data allows to judge which glycosylation is reliable (Figures 2 and 6). Unfortunately, peptides of $KLK3_{S/T}$ from both tryptic and chymotryptic digest were not resolved in these measurements, most likely due to the presence of inhomogeneous *N*-glycosylation at Asn61. This single glycosylation site may carry mannose-rich hybrid glycans and a mixture of bi- and triantennary *N*-glycans with varying numbers of fucose and terminal sialic acids that were observed for KLK3, similar to mammalian KLK4 (Figure 1C) (Sarrats et al., 2010; Stura et al., 2011; Yamakoshi et al., 2011; Ishikawa et al., 2017). Nevertheless, the high molecular weight on SDS gels and downshifts upon enzymatic deglycosylation confirm the *N*-glycosylation of $KLK3_{S/T}$. Regarding KLK4, the expected *N*-glycosylation at Asn159 appears to be much more reliable (Figure 2B). The lack of deglycosylation of $KLK4_{lx}$ by Endo Hf might depend on slightly extended core *N*-glycans, which could carry a fucose and two Gal-Sia antennae (Breitling et al., 2002). In general, *Leishmania* are capable of the unusual posphoserine-*O*-glycosylation, while common *O*-glycosylation of human proteins in *L. tarentolae* was recently confirmed (Ilg et al., 1994; Klatt et al., 2013). Among the four sequons of $KLK11_{lx}$, the one Asn202 is most likely linked to a $GlcNAc_2Man_3$ core glycan, however, Asn159, Asn175 and in particular Asn95 might be incompletely occupied. Moreover, these *N*-glycans seem to be extended by up to two sugars. The partial *O*-glycosylation of Ser95b, Thr161, Thr177, and Ser204 is less reliable according to the MS analysis, while the O-glycan masses could be comparable to core glycans, which would explain the high apparent molecular weight of 36 kDa for $KLK11_{lx}$ on SDS polyacrylamide gels (Figure 2A).

Although the activation assays for pro-KLK4 and pro-KLK11 were not as systematic as in previous studies, they focus on the physiological set of prostatic KLKs with native-like glycosylation (Yoon et al., 2007, 2009; Beaufort et al., 2010). Remarkably, glycosylated $KLK2_{lx}$ was most efficient in cleaving the propeptide SCSQ from pro-KLK4, which does not match the known specificity profiles of $KLK2_e$ and $KLK2_{lx}$ with P1-Gln as disfavored residue (Skala et al., 2013; Guo et al., 2016). Otherwise, the results for pro-KLK11 activation with the propetide ETR are similar to the one reported for propeptide fusion proteins (Yoon et al., 2007). The native-like pro-KLK4 activation experiment clearly demonstrates that not only the three-dimensional protein structures of enzyme and substrate have to be considered, but also their distinct post-translational modifications, such as glycosylation (Figure 3A). Additional molecular properties of KLK4 could play role in the interaction with KLK2, such as the negatively charged patch in the region of the usually positively charged patch of thrombin and several KLKs, termed 'anion binding exosite I' (Debela et al., 2008). KLK2 may bind this region in a preferential manner, resulting in activation of pro-KLK4 despite the unfavorable P1-Gln. Thus, the 3D-structure derived tertiary specificity of a protease is an additional level of information, which is required for a full understanding of physiological and pathological processes.

The conformation of a protein structure, as a whole or in parts of it, can be significantly influenced by glycosylation. Thus, it is not surprising that the glycosylated and glycan-free KLKs exhibit slightly different enzyme kinetic parameters, such as a roughly doubled k_{cat} of glycosylated $KLK4_{lx}$ and $KLK11_{lx}$ compared with the values of the glycan-free counterparts (Figure 4A and Table 1). Depending on the higher k_{cat}, the catalytic efficiency was enhanced, probably based on a conformational optimization of the active site, as it was observed for the cleavage of large protein substrates by $KLK2_{lx}$ compared with $KLK2_e$ (Guo et al., 2016). Even if a glycan does not directly influence the active site as in $KLK2_{lx}$, more distant, functionally connected amino acid positions could explain the enzyme kinetic differences according to the concept of protein sectors (Halabi et al., 2009). The *N*-glycosylated Asn159 of $KLK4_{lx}$ and $KLK11_{lx}$ would be positioned right between the structural core sector, Cys157 and the S1 pocket surrounding sector at residue 161, if the analogy to rat trypsin is valid. Seemingly, the strong difference of Zn^{2+} inhibition with respect to the residual activity depends on the single glycan linked to Asn159 $KLK4_{lx}$. Interestingly, a residual activity of 25% was observed for $KLK4_e$ even at 1 mM Zn^{2+}, whereby the Zn^{2+}-binding site was unambiguously identified at His25 and Glu77 (Debela et al., 2006a). However, these samples were pre-treated with mM Ca^{2+}, in order to maintain a monomeric state of KLK4, which tends to oligomerize and lose activity. Glycosylation at Asn159 could prevent the formation of higher KLK4 oligomers, but it is compatible with tetramers and octamers (PDB code 2BDI).

The degradation of the natural substrate fibronectin by glycosylated $KLK3_{S/T}$ and $KLK4_{T/lx}$ shows no significant differences (Figure 5A). Only a comparison with glycan-free KLKs 3 and 4 might demonstrate effects of glycosylation on activity, which seems rather unlikely, as the glycans of both KLKs are located distant to the active site cleft (Figures 1 and 2B). The tryptic $KLK11_{lx}$ hardly cleaved

fibronectin, which confirmed an earlier study on KLK11 from seminal plasma (Luo et al., 2006). This finding can be explained by the specific three-dimensional architecture of substrate and protease, e.g. by altered exosite interactions or the influence of glycans. Remarkably, the ternary complex of the serpin antithrombin with thrombin and a bridging heparin corroborates that *N*-glycans of both protein molecules can serve as additional determinants of the heparin binding mode (Li et al., 2004). Noteworthy, KLK3 binds heparin as well and Asn61 is located similar to Asn60G of thrombin, which agrees with a similar role in the heparin enhanced complex formation of KLK3 with PCI (Christensson and Lilja, 1994).

Regardless of potential functional roles, a major structural and concomitantly regulatory role of the glycans is long-term stabilization, most likely by protection of sensitive cleavage sites (Figure 6A and B). This concept was confirmed for glycosylated $KLK2_{lx}$ and is further supported by the higher fractions of active glycosylated $KLK3_{S}$, $KLK4_{lx}$ and $KLK11_{lx}$, which are around 50% according to active site titrations, compared to their glycan-free counterparts, which are only active around 10% on average (Guo et al., 2016). An additional role in regulation of enzyme activity for the *N*-linked Glycan at Asn95 of KLK2 was described by Guo et al. (2016). Apart from the physiological roles of glycosylation, aberrant glycosylation of prostatic KLKs in cancer deserves future investigations, which might improve the detection of aggressive forms by glycan analysis of KLK3 and could be supported by corresponding analyses of the three other prostatic KLKs. In addition, the glycosylation patterns of all KLKs expressed under pathological conditions could help to target them in diagnostic and therapeutic approaches.

Materials and methods

Cloning and expression of glycosylated prostatic KLKs

Similar cloning and expression procedures for glycosylated $KLK2_{lx}$ have been published previously (Guo et al., 2016). All constructs for native-like proforms and mature KLKs 3, 4 and 11 require artificial propeptides for purification with His-tags and prevention of autodegradation. For mature KLKs, the EK recognition sequence His_6-GS-DDDDK- was introduced, preceding Ile16 of the mature proteases. For pro KLKs 3 and 4 TEV protease cleavage sites His_6-GS-ENLYFQG-A/S were used, while the AEP cleavage site was His_6-GS-N- for KLK11 (Dando et al., 1999; Kapust et al., 2002). Encoding DNA fragments were amplified by polymerase chain reaction (PCR) using appropriate primers with XbaI and NotI for N-terminal His-tags or KpnI restriction sites for C-terminal His-tags, respectively. PCR products were inserted into the pLEXSY-sat2 vector (Jena Bioscience, Jena, Germany) following the established protocols (Breitling et al., 2002; Guo et al., 2016).

For transient secretory expression in HEK293 cells, encoding DNA fragments of KLKs were amplified by PCR and inserted into the mammalian expression vector pHLsec (Aricescu et al., 2006) at AgeI and XhoI restriction sites for N-terminal His-tags or AgeI and KpnI for C-terminal His-tag fusion proteins. HEK293 cells were grown in a humidified 37°C incubator with 5% CO_2 in Dulbecco's Modified Eagle's Medium (DMEM) containing 2 mM L-glutamine, non-essential amino-acids (NEAA) and 10% fetal bovine serum (FBS, Invitrogen, Karlsruhe, Germany) in T-175 tissue culture flasks (Greiner, Frickenhausen, Germany). Adherent HEK293 cells were detached with 80% confluent using 1× trypsin/EDTA followed by PBS wash, and then passaged at a ratio of 1:10–1:20 for general maintenance. For expression, the HEK293 cells were cultivated to confluence 80% and transfected with cDNA encoding prostatic KLKs with polyethylenimine (PEI, Sigma, Munich, Germany) at a weight ratio for DNA:PEI of 1:1.5. Transfected cells were cultivated in DMEM medium containing 2% FBS, L-glutamine and NEAA. Secreted protein was detected by immunoblots of conditioned media with a penta-His antibody. Large-scale cultures for protein expression were performed in an expanded-surface polystyrene roller bottle (2280 cm^2, Greiner Bio-One, Frickenhausen, Germany). When the media color change from pink-red to yellow, the supernatants were collected and refilled with new condition media, repeated twice to maximize the production of secreted prostatic KLKs.

Protein purification including generation of correct N-termini

Secreted His-tagged KLKs were purified from the supernatant medium after centrifugation of the cells (4500 rpm, 30 min) with incubation on Ni-NTA resin (Qiagen Inc., Valencia, CA, USA) at 4°C for 4 h or overnight in case of LEXSY cells. In the case of HEK293 cells, this was preceded by filtration through 0.45 µm polyether sulfone (PES) membranes and dialysis against 1000 times excess of 100 mM NaCl, 5% glycerol, 20 mM Tris/HCl, pH 8.0, in order to remove the 66 mM Ca^{2+} from the culture media, which would reduce the IMAC efficiency. Proforms of KLKs were eluted from Ni-NTA resin with 50 mM imidazole in the same buffer.

Mature KLK constructs with the artificial propeptides DDDDK were treated with C-terminally His-tagged EK, generating the correct N-terminus for activation pocket of trypsin-like serine proteases (Skala et al., 2013). Recombinant KLKs were activated by EK at molar ratios of 50:1–1000:1 at room temperature overnight. Cleavage of the pro-KLK11 construct at the AEP recognition site His_6-GS-N-ETR-I16 was performed at pH 4.5–5.5 at a ratio of 50:1. The more specific TEV protease cleaves at small, unbranched P1′ residues as in the KLK3 and KLK4 constructs His_6-GS-ENLYFQG-APLILSR-I^{16} or -SCSQ-I^{16} (Kapust et al., 2002). Instead of DTT, which could reduce disulfides, a glutathione redox buffer was used, which maintains reducing conditions for TEV protease. The reactions were performed with a 5:1 ratio of KLK fusion proteins to TEV at room temperature in 50 mM Tris/HCl (pH 8.0), 0.5 mM EDTA, 3 mM reduced glutathione and 0.3 mM oxidized glutathione.

Uncleaved fusion proteins with N-terminal His-tags, as well as the artificial propeptides with His-tags and C-terminally His-tagged EK were removed by chromatography on Ni-NTA columns (GE Healthcare, Munich, Germany). Imidazole was removed by dialysis against 50 mM Tris/HCl (pH 8.0), 500 mM NaCl in 6–8 kDa cutoff membranes

(Spectra/Por, Spectrum Labs, Rancho Dominguez, CA, USA). The His-tagged molecules were removed by Ni-NTA columns from target proteins. Additional purification of KLKs 4 and 11 with trypsin-like specificity, was achieved by benzamidine sepharose columns in 50 mM Tris/HCl (pH 8.0), 500 mM NaCl as loading and wash buffer. KLKs were eluted in this buffer plus 100 mM benzamidine or 20 mM *p*-amino-benzamidine or 0.5 M arginine (pH 3.0). For size exclusion chromatography (SEC), samples were concentrated to 500 µl with 10 kDa cutoff centrifugal filters (Amicon, Millipore, Billerica, MA, USA). Usually, SEC on Superdex 75 10/300 GL columns (GE Healthcare, Munich, Germany) in 100 mM NaCl, 5% glycerol, 20 mM Tris/HCl (pH 8.0), resulted in >95% pure and homogeneous samples.

Glycan characterization

The periodic acid-Schiff (PAS) reaction was used for the detection of glycosylated proteins, which was successful for $KLK2_{lx}$ (Guo et al., 2016). The sensitivity is 25–100 ng glycoprotein, while the reagent GlycoProfile III and PVDF membranes increased the detection limits. Recombinant KLKs were separated by 15% SDS-PAGE and transferred to nitrocellulose membranes in semidry Western blots, followed by 5 min wash and incubation in 1% periodic acid/3% acetic acid 15 min in the dark. After washing with H_2O (5 min, three times), the membrane was developed with the Schiff reagent, resulting in magenta staining after 3–10 min. Rinsing with water (5 min) and air-drying fixed the membranes permanently.

Enzymatic deglycosylation under denaturing conditions was performed following the instructions of the enzyme producer New England Biolabs (Frankfurt a. M., Germany). Ten micrograms of prostatic KLK sample were treated with 500 units of PNGase F in 50 mM sodium phosphate, pH 7.5 or with 1000 units of Endo Hf in 50 mM sodium acetate pH 6.0 at 37°C for 1 h. Reactions were terminated with sample buffer and products were monitored by SDS-PAGE.

For mass spectrometry, 50 µg purified pro-KLK3/4/11 from LEXSY or HEK293S/T cells stored in a freezer before the test. The thawed solution was digested either by trypsin or by chymotrypsin and the proteolytic fragments were sequenced by means of tandem mass spectrometry with a Q-Exactive LC-MS/MS system (Thermo Scientific, Dreieich, Germany). Data analysis was performed with PEAKS Studio version 7.0 (Bioinformatics Solutions, Waterloo, ON, Canada), a *de novo* sequencing program that also considers mass shifts caused by amino acid modifications. This makes it possible to deduce modification sites from peptide fragment spectra in a reliable manner.

Pro-KLK fusion protein hydrolysis and enzymatic assays

The ability of prostate-specific KLKs to convert individual pro-KLKs into enzymatic active species was assessed by incubation of 10 µg pro-KLK fusion protein with 0.1 µg KLK protease in 150 mM NaCl, 10 mM Tris/HCl (pH 8.0) at 37°C for 24 h. The reactions were stopped on ice and samples prepared for SDS-PAGE and activity assays. The activation of pro-KLKs by KLK proteases was evaluated with 1 mM fluorogenic H-PFR-AMC, which was measured in an Infinite M200 microplate reader (Tecan, Männedorf, Switzerland) with wavelengths of 380 nm (excitation) and 460 nm (emission). The fluorescence intensity generated by activated pro-KLKs was compared to control samples of pro-KLKs without activating protease, protease alone and buffer. Relative turnover velocities were calculated with the highest velocity defined as 100%, considering 10% as suitable cutoff for activation.

All para-nitroanilide (pNA) and 7-amino-4-methylcoumarin (AMC) substrates and the inhibitors D-phenylalanyl-L-prolyl-L-arginine chloromethyl ketone (PPACK) and carboxy-benzyl-L-leucyl-L-tyrosine chloromethyl ketone (Z-LY-cmk) were purchased from Bachem (Weil am Rhein, Germany) and stock solutions were prepared in DMSO. For enzymatic assays in 100 µl samples with 50 mM Tris/HCl (pH 7.5), 100 mM NaCl at 37°C with 0.1% (w/v) BSA were used, which was replaced by 0.005% Tween-20 for enzyme kinetic measurements in 50 µl samples. Protein concentrations were measured with a NanoDrop 2000c spectrophotometer (Thermo Scientific, Dreieich, Germany) at 280 nm, using computed extinction coefficients. Released pNA was recorded photometrically at 405 nm on the Infinite M200 microplate reader. Standard curves of pNA and AMC (Sigma, Munich, Germany) were measured under identical conditions as the assays and used in calculating the rate of product formation, i.e. the turnover velocity.

The initial velocity of turnover was measured in triplicates in the range of 20 µM–5 mM substrate with an enzyme concentration of 500 nM. Data were fitted to the Michaelis-Menten equation by nonlinear regression analysis to obtain V_{max} and K_M, performed with the ORIGIN software (Origin Lab, Northampton, MA, USA). The fraction of active protease was determined with suitable chromogenic substrates by active site titration after 30 min incubation with the irreversible inhibitor PPACK for tryptic KLKs, while KLK3 was titrated with Z-LY-cmk (Myles et al., 2001; Skala et al., 2014; Guo et al., 2016). After calculation of k_{cat} values, the standard deviation for k_{cat}/K_M was calculated according to Fenner (Fenner, 1931). Zn^{2+} inhibition curves were measured in assay buffer (pH 7.0) with 0.005% Tween-20.

Interaction with protein substrates and inhibitors

For fibronectin degradation, 50 µg human serum fibronectin (Innovative research, Novi, MI, USA) was incubated with 0.5 µg tryptic KLKs or 2.5 µg KLK3 for 0, 1, 2, 4 and 24 h at 37°C in 50 mM Tris/HCl, pH 8.0, containing 0.1% NP40, 150 mM NaCl. An equal amount of fibronectin or protease alone was monitored under identical conditions as a control. The covalent bond formation of KLKs with serpins or A2M was evaluated by SDS-gels. Six micrograms A2M were incubated with 1.3 µg KLK at 37°C for 1 h in 150 mM NaCl, 20 mM Tris/HCl (pH 8.0). Similarly, the interaction of protease with 5.7 µg PCI or 4.5 µg anti-chymotrypsin was tested under the same condition, with a molar ratio of inhibitor to protease of 2:1. An equal amount of inhibitor or protease alone was monitored as control.

Acknowledgments: We are thankful to Sabine Creutzburg for molecular biological work and Reinhard Mentele for N-terminal sequencing. In addition, we would like to thank Wolfgang Skala for providing KLKs from *E. coli* expression. This study was supported by the Austrian Science Fund (FWF) with D-A-CH project, Funder Id: 10.13039/501100002428, I631-B11 and W_01213 (S.G.) as well as with project P25003-B21 (P.G.). The German Research Foundation (DFG) contributed with financial support from Funder Id: 10.13039/501100001659, grant MA 1236-10-1 (V.M.).

References

Aebi, M. (2013). N-linked protein glycosylation in the ER. Biochim. Biophys. Acta *1833*, 2430–2437.

Andrade, D., Assis, D.M., Lima, A.R., Oliveira, J.R., Araujo, M.S., Blaber, S.I., Blaber, M., Juliano, M.A., and Juliano, L. (2010). Substrate specificity and inhibition of human kallikrein-related peptidase 3 (KLK3 or PSA) activated with sodium citrate and glycosaminoglycans. Arch. Biochem. Biophys. *498*, 74–82.

Apweiler, R., Hermjakob, H., and Sharon, N. (1999). On the frequency of protein glycosylation, as deduced from analysis of the Swiss-Prot database. Biochim. Biophys. Acta *1473*, 4–8.

Aricescu, A.R., Lu, W., and Jones, E.Y. (2006). A time- and cost-efficient system for high-level protein production in mammalian cells. Acta Crystallogr. D Biol. Crystallogr. *62*, 1243–1250.

Avgeris, M., Mavridis, K., and Scorilas, A. (2012). Kallikrein-related peptidases in prostate, breast, and ovarian cancers: from pathobiology to clinical relevance. Biol. Chem. *393*, 301–317.

Beaufort, N., Debela, M., Creutzburg, S., Kellermann, J., Bode, W., Schmitt, M., Pidard, D., and Magdolen, V. (2006). Interplay of human tissue kallikrein 4 (hk4) with the plasminogen activation system: Hk4 regulates the structure and functions of the urokinase-type plasminogen activator receptor (uPAR). Biol. Chem. *387*, 217–222.

Beaufort, N., Plaza, K., Utzschneider, D., Schwarz, A., Burkhart, J., Creutzburg, S., Debela, M., Schmitt, M., Ries, C., and Magdolen, V. (2010). Interdependence of kallikrein-related peptidases in proteolytic networks. Biol. Chem. *391*, 581–587.

Breitling, R., Klingner, S., Callewaert, N., Pietrucha, R., Geyer, A., Ehrlich, G., Hartung, R., Müller, A., Contreras, R., Beverley, S.M., et al. (2002). Non-pathogenic trypanosomatid protozoa as a platform for protein research and production. Protein Expr. Purif. *25*, 209–218.

Christensson, A. and Lilja, H. (1994). Complex formation between protein c inhibitor and prostate-specific antigen *in vitro* and in human semen. Eur. J. Biochem. *220*, 45–53.

Christensson, A., Laurell, C.-B., and Lilja, H. (1990). Enzymatic activity of prostate-specific antigen and its reactions with extracellular serine proteinase inhibitors. Eur. J. Biochem. *194*, 755–763.

Cloutier, S.M., Chagas, J.R., Mach, J.-P., Gygi, C.M., Leisinger, H.-J., and Deperthes, D. (2002). Substrate specificity of human kallikrein 2 (hK2) as determined by phage display technology. Eur. J. Biochem. *269*, 2747–2754.

Dando, P., Fortunato, M., Smith, L., Knight, C., Mckendrick, J., and Barrett, A. (1999). Pig kidney legumain: an asparaginyl endopeptidase with restricted specificity. Biochem. J. *339*, 743–749.

Debela, M., Magdolen, V., Grimminger, V., Sommerhoff, C., Messerschmidt, A., Huber, R., Friedrich, R., Bode, W., and Goettig, P. (2006a). Crystal structures of human tissue kallikrein 4: activity modulation by a specific zinc binding site. J. Mol. Biol. *362*, 1094–1107.

Debela, M., Magdolen, V., Schechter, N., Valachova, M., Lottspeich, F., Craik, C.S., Choe, Y., Bode, W., and Goettig, P. (2006b). Specificity profiling of seven human tissue kallikreins reveals individual subsite preferences. J. Biol. Chem. *281*, 25678–25688.

Debela, M., Goettig, P., Magdolen, V., Huber, R., Schechter, N.M., and Bode, W. (2007). Structural basis of the zinc inhibition of human tissue kallikrein 5. J. Mol. Biol. *373*, 1017–1031.

Debela, M., Beaufort, N., Magdolen, V., Schechter, N.M., Craik, C.S., Schmitt, M., Bode, W., and Goettig, P. (2008). Structures and specificity of the human kallikrein-related peptidases KLK 4, 5, 6, and 7. Biol. Chem. *389*, 623–632.

Drake, R.R., Jones, E.E., Powers, T.W., and Nyalwidhe, J.O. (2015). Altered glycosylation in prostate cancer. In: Advances in cancer research, R.R. Drake and L.E. Ball, eds. (Cambridge, MA, USA: Academic Press), pp. 345–382.

Emami, N. and Diamandis, E.P. (2012). Kallikrein-related peptidases and semen. In: Kallikrein-related peptidases, V. Magdolen, P. Sommerhoff Christian, H. Fritz, and M. Schmitt, eds. (Berlin: De Gruyter), pp. 311–327.

Engh, R.A., Brandstetter, H., Sucher, G., Eichinger, A., Baumann, U., Bode, W., Huber, R., Poll, T., Rudolph, R., and Von Der Saal, W. (1996). Enzyme flexibility, solvent and 'weak' interactions characterize thrombin-ligand interactions: implications for drug design. Structure *4*, 1353–1362.

España, F., Navarro, S., Medina, P., Zorio, E., and Estellés, A. (2007). The role of protein c inhibitor in human reproduction. Semin. Thromb. Hemost. *33*, 041–045.

Fenner, G. (1931). The measure of accuracy of sums, products and quotients of measurement series. Naturwissenschaften *19*, 310–310.

Freeze, H.H. and Kranz, C. (2010). Endoglycosidase and glycoamidase release of n-linked glycans. In: Current protocols in molecular biology, F.M. Ausubel, R.B. Robert, E. Kingston, D.D. Moore, J.G. Seidman, J.A. Smith and K. Struhl, eds. (Hoboken, NJ, USA: John Wiley & Sons, Inc.).

Fuhrman-Luck, R.A., Loessner, D., and Clements, J.A. (2014). Kallikrein-related peptidases in prostate cancer: from molecular function to clinical application. EJIFCC *25*, 269–281.

Fuhrman-Luck, R.A., Stansfield, S.H., Stephens, C.R., Loessner, D., and Clements, J.A. (2016). Prostate cancer-associated kallikrein-related peptidase 4 activates matrix metalloproteinase-1 and thrombospondin-1. J. Proteome Res. *15*, 246–2478.

Gilgunn, S., Conroy, P.J., Saldova, R., Rudd, P.M., and O'kennedy, R.J. (2013). Aberrant PSA glycosylation – a sweet predictor of prostate cancer. Nat. Rev. Urol. *10*, 99–107.

Goettig, P. (2016). Effects of glycosylation on the enzymatic activity and mechanisms of proteases. Int. J. Mol. Sci. *17*, 1969.

Guo, S., Skala, W., Magdolen, V., Brandstetter, H., and Goettig, P. (2014). Sweetened kallikrein-related peptidases (klks): glycan trees as potential regulators of activation and activity. Biol. Chem. *395*, 959–976.

Guo, S., Skala, W., Magdolen, V., Briza, P., Biniossek, M.L., Schilling, O., Kellermann, J., Brandstetter, H., and Goettig, P. (2016). A single glycan at the 99-loop of human kallikrein-related peptidase 2 regulates activation and enzymatic activity. J. Biol. Chem. *291*, 593–604.

Gupta, A., Roobol, M.J., Savage, C.J., Peltola, M., Pettersson, K., Scardino, P.T., Vickers, A.J., Schröder, F.H., and Lilja, H. (2010). A four-kallikrein panel for the prediction of repeat prostate biopsy: data from the european randomized study of prostate cancer screening in rotterdam, netherlands. Br. J. Cancer *103*, 708.

Halabi, N., Rivoire, O., Leibler, S., and Ranganathan, R. (2009). Protein sectors: evolutionary units of three-dimensional structure. Cell *138*, 774–786.

Harvey, T.J., Hooper, J.D., Myers, S.A., Stephenson, S.A., Ashworth, L.K., and Clements, J.A. (2000). Tissue-specific expression pat-

terns and fine mapping of the human kallikrein (*KLK*) locus on proximal 19q13.4. J. Biol. Chem. *275*, 37397–37406.

Hong, S.K. (2014). Kallikreins as biomarkers for prostate cancer. BioMed. Res. Int. *2014*, 10.

Hsieh, M.-C. and Cooperman, B.S. (2000). The preparation and catalytic properties of recombinant human prostate-specific antigen (rpsa). Biochim. Biophys. Acta Protein Struct. Mol. Enzymol. *1481*, 75–87.

Ilg, T., Overath, P., Ferguson, M.A., Rutherford, T., Campbell, D.G., and Mcconville, M.J. (1994). O- and n-glycosylation of the *Leishmania mexicana*-secreted acid phosphatase. Characterization of a new class of phosphoserine-linked glycans. J. Biol. Chem. *269*, 24073–24081.

Ishikawa, T., Yoneyama, T., Tobisawa, Y., Hatakeyama, S., Kurosawa, T., Nakamura, K., Narita, S., Mitsuzuka, K., Duivenvoorden, W., Pinthus, J., et al. (2017). An automated micro-total immunoassay system for measuring cancer-associated α2,3-linked sialyl N-glycan-carrying prostate-specific antigen may improve the accuracy of prostate cancer diagnosis. Int. J. Mol. Sci. *18*, 470.

Kapust, R.B., Tözsér, J., Copeland, T.D., and Waugh, D.S. (2002). The p1′ specificity of tobacco etch virus protease. Biochem. Biophys. Res. Commun. *294*, 949–955.

Karakosta, T.D., Soosaipillai, A., Diamandis, E.P., Batruch, I., and Drabovich, A.P. (2016). Quantification of human kallikrein-related peptidases in biological fluids by multiplatform targeted mass spectrometry assays. Mol. Cell Proteomics *15*, 2863–2876.

Kellermann, J., Lottspeich, F., Geiger, R., and Deutzmann, R. (1988). Human urinary kallikrein-amino acid sequence and carbohydrate attachment sites. Protein Seq. Data Anal. *1*, 177–182.

Klatt, S., Rohe, M., Alagesan, K., Kolarich, D., Konthur, Z., and Hartl, D. (2013). Production of glycosylated soluble amyloid precursor protein α (sappalpha) in *Leishmania tarentolae*. J. Proteome Res. *12*, 396–403.

Kuriyama, M., Wang, M.C., Lee, C.-L., Papsidero, L.D., Killian, C.S., Inaji, H., Slack, N.H., Nishiura, T., Murphy, G.P., and Chu, T.M. (1981). Use of human prostate-specific antigen in monitoring prostate cancer. Cancer Res. *41*, 3874–3876.

Li, W., Johnson, D.J.D., Esmon, C.T., and Huntington, J.A. (2004). Structure of the antithrombin-thrombin-heparin ternary complex reveals the antithrombotic mechanism of heparin. Nat. Struct. Mol. Biol. *11*, 857–862.

Lovgren, J., Rajakoski, K., Karp, M., Lundwall, A., and Lilja, H. (1997). Activation of the zymogen form of prostate-specific antigen by human glandular kallikrein 2. Biochem. Biophys. Res. Commun. *238*, 549–555.

Luo, L.Y., Shan, S.J., Elliott, M.B., Soosaipillai, A., and Diamandis, E.P. (2006). Purification and characterization of human kallikrein 11, a candidate prostate and ovarian cancer biomarker, from seminal plasma. Clin. Cancer Res. *12*, 742–750.

Malm, J., Hellman, J., Hogg, P., and Lilja, H. (2000). Enzymatic action of prostate-specific antigen (PSA or HK3): substrate specificity and regulation by Zn^{2+}, a tight-binding inhibitor. Prostate *45*, 132–139.

Matsumura, M., Bhatt, A.S., Andress, D., Clegg, N., Takayama, T.K., Craik, C.S., and Nelson, P.S. (2005). Substrates of the prostate-specific serine protease prostase/KLK4 defined by positional-scanning peptide libraries. Prostate *62*, 1–13.

Myles, T., Yun, T.H., Hall, S.W., and Leung, L.L.K. (2001). An extensive interaction interface between thrombin and factor V is required for factor V activation. J. Biol. Chem. *276*, 25143–25149.

Padler-Karavani, V. (2014). Aiming at the sweet side of cancer: aberrant glycosylation as possible target for personalized-medicine. Cancer Lett. *352*, 102–112.

Papsidero, L.D., Wang, M.C., Valenzuela, L.A., Murphy, G.P., and Chu, T.M. (1980). A prostate antigen in sera of prostatic cancer patients. Cancer Res. *40*, 2428–2432.

Peracaula, R., Tabares, G., Royle, L., Harvey, D.J., Dwek, R.A., Rudd, P.M., and De Llorens, R. (2003). Altered glycosylation pattern allows the distinction between prostate-specific antigen (PSA) from normal and tumor origins. Glycobiology *13*, 457–470.

Reid, J.C., Matsika, A., Davies, C.M., He, Y., Broomfield, A., Bennett, N.C., Magdolen, V., Srinivasan, B., Clements, J.A., and Hooper, J.D. (2017). Pericellular regulation of prostate cancer expressed kallikrein-related peptidases and matrix metalloproteinases by cell surface serine proteases. Am. J. Cancer Res. *7*, 2257–2274.

Sarrats, A., Saldova, R., Comet, J., O'donoghue, N., De Llorens, R., Rudd, P.M., and Peracaula, R. (2010). Glycan characterization of PSA 2-de subforms from serum and seminal plasma. OMICS *14*, 465–474.

Shaw, J.L.V. and Diamandis, E.P. (2007). Distribution of 15 human kallikreins in tissues and biological fluids. Clin. Chem. *53*, 1423–1432.

Skala, W., Goettig, P., and Brandstetter, H. (2013). Do-it-yourself histidine-tagged bovine enterokinase: a handy member of the protein engineer's toolbox. J. Biotechnol. *168*, 421–425.

Skala, W., Utzschneider, D.T., Magdolen, V., Debela, M., Guo, S., Craik, C.S., Brandstetter, H., and Goettig, P. (2014). Structure-function analyses of human kallikrein-related peptidase 2 establish the 99-loop as master regulator of activity. J. Biol. Chem. *289*, 34267–34283.

Sotiropoulou, G., Pampalakis, G., and Diamandis, E.P. (2009). Functional roles of human kallikrein-related peptidases. J. Biol. Chem. *284*, 32989–32994.

Stenman, U.-H., Leinonen, J., Alfthan, H., Rannikko, S., Tuhkanen, K., and Alfthan, O. (1991). A complex between prostate-specific antigen and α1-antichymotrypsin is the major form of prostate-specific antigen in serum of patients with prostatic cancer: assay of the complex improves clinical sensitivity for cancer. Cancer Res. *51*, 222–226.

Stephan, C., Jung, K., Lein, M., and Diamandis, E.P. (2007). PSA and other tissue kallikreins for prostate cancer detection. Eur. J. Cancer *43*, 1918–1926.

Stura, E.A., Muller, B.H., Bossus, M., Michel, S., Jolivet-Reynaud, C., and Ducancel, F. (2011). Crystal structure of human prostate-specific antigen in a sandwich antibody complex. J. Mol. Biol. *414*, 530–544.

Tabares, G., Radcliffe, C.M., Barrabes, S., Ramirez, M., Aleixandre, R.N., Hoesel, W., Dwek, R.A., Rudd, P.M., Peracaula, R., and De Llorens, R. (2006). Different glycan structures in prostate-specific antigen from prostate cancer sera in relation to seminal plasma psa. Glycobiology *16*, 132–145.

Uhlén, M., Fagerberg, L., Hallström, B.M., Lindskog, C., Oksvold, P., Mardinoglu, A., Sivertsson, Å., Kampf, C., Sjöstedt, E., Asplund, A., et al. (2015). Tissue-based map of the human proteome. Science *347*, 1260419.

Watt, K.W., Lee, P.J., M'timkulu, T., Chan, W.P., and Loor, R. (1986). Human prostate-specific antigen: structural and functional similarity with serine proteases. Proc. Natl. Acad. Sci. USA *83*, 3166–3170.

Yamakoshi, Y., Yamakoshi, F., Hu, J.C.C., and Simmer, J.P. (2011). Characterization of kallikrein-related peptidase 4 glycosylations. Eur. J. Oral Sci. *119*, 234–240.

Yoneyama, T., Ohyama, C., Hatakeyama, S., Narita, S., Habuchi, T., Koie, T., Mori, K., Hidari, K.I.P.J., Yamaguchi, M., Suzuki, T., et al. (2014). Measurement of aberrant glycosylation of prostate specific antigen can improve specificity in early detection of prostate cancer. Biochem. Bioph. Res. Commun. *448*, 390–396.

Yoon, H., Laxmikanthan, G., Lee, J., Blaber, S.I., Rodriguez, A., Kogot, J.M., Scarisbrick, I.A., and Blaber, M. (2007). Activation profiles and regulatory cascades of the human kallikrein-related peptidases. J. Biol. Chem. *282*, 31852–31864.

Yoon, H., Blaber, S.I., Debela, M., Goettig, P., Scarisbrick, I.A., and Blaber, M. (2009). A completed KLK activome profile: investigation of activation profiles of KLK9, 10 and 15. Biol. Chem. *390*, 373–377.

Zhang, W.M., Leinonen, J., Kalkkinen, N., Dowell, B., and Stenman, U.H. (1995). Purification and characterization of different molecular forms of prostate-specific antigen in human seminal fluid. Clin. Chem. *41*, 1567–1573.

Zielinska, D.F., Gnad, F., Wiśniewski, J.R., and Mann, M. (2010). Precision mapping of an *in vivo* N-glycoproteome reveals rigid topological and sequence constraints. Cell *141*, 897–907.